Proceedinsg of the Second International Symposium on Therapeutic Ultrasound, Seattle, WA, July 2002.

Bubbles and HIFU: The Good, the Bad, and the Ugly

R. Glynn Holt, Ronald A. Roy, Patrick A. Edson, Xinmai Yang

Boston University, Department of Aerospace and Mechanical Engineering
Boston, MA 02215

Abstract. Rapid hyperthermia resulting in tissue necrosis has proven to be a useful therapeutic modality for clinical application of high-intensity focused ultrasound. At therapeutic intensities, the hyperthermia is often accompanied by bubble activity. In vitro and in vivo experiments alike have shown that under certain conditions bubble activity can give rise to a doubling of the heating rate. With a view towards harnessing the energy-concentrating effects of bubbles to do useful clinical work, we report the results of experiments and modeling for the dynamic and thermal behavior of bubbles subjected to 1-megahertz ultrasound at megapascal pressures. The dominant heating mechanism depends on bubble size, medium shear viscosity number and frequency-dependent acoustic attenuation. The bubble size distribution, in turn, depends on insonation control parameters (acoustic pressure, pulse duration), medium properties (notably dissolved gas concentration) and bubble-destroying shape instabilities. The evidence obtained so far points to a range of control parameters for which bubble-enhanced heating can be assured.
[Work supported by DARPA and the U.S. Army]

BUBBLES AND HIFU: BACKGROUND AND MOTIVATION

Acoustic cavitation (the acoustically induced nucleation and subsequent oscillatory activity of bubbles) is often the result of the application of ultrasound in a biomedical context. There are sound reasons, both experimental and theoretical, for defining therapeutic and diagnostic operating conditions in order to minimize bubble activity (Williams et al. 1991; Carstensen et al. 1993; Penney et al. 1993; Everbach et al. 1997). Most of the arguments boil down to the fact that bubbles perform a very efficient and highly nonlinear conversion of acoustical energy to mechanical motion. In diagnostic ultrasound, the Mechanical Index (MI) was conceived and implemented because of the perceived risk of mechanical bioeffects from the violent inertial collapses of bubbles (Apfel and Holland 1991). In therapeutic ultrasound, bubbles formed in the propagation path inhibit deposition of acoustic energy because they scatter and absorb much of the energy before it can reach the target area, a process often referred to as 'screening' or 'shielding'.

Conversely, there are often diagnostic situations in which the use of bubble-based contrast agents make cavitation activity unavoidable (Fowlkes and Holland 2000), and therapeutic situations in which it is desirable to excite cavitation. Such is the case in the field of ultrasound surgery using high-intensity focused ultrasound (HIFU), where the goal is to produce irreversible necrosis deep into the tissue with

minimal damage in the intervening path (as reviewed in ter Haar 1995, and highlighted in the special issue of IEEE UFFC, November 1996). The fact that bubbles enhance ultrasound imaging via their high backscatter cross section makes them useful in targeting applications. If gross mechanical damage and tissue ablation is desired, then excitation of cavitation bubbles is the most efficacious (if also unavoidable) method at high insonation pressures and long insonation durations (for example, Fry et al. 1950; Lehmann and Herrick 1953; Fry et al. 1970; ter Haar et al. 1982; Fry et al. 1996; Tavakkoli 1997; Arefiev et al. 1998, Smith and Hynynen 1998).

However, if controlled, highly localized hyperthermia is the desired outcome, then most investigators have argued that cavitation is to be avoided, since it has typically led to unpredictable thermal results. Several authors observe irregular lesions and collateral damage outside the focal zone when uncontrolled cavitation occurs during insonation (Fry et al. 1970; Lele 1987; Hynynen 1991; Chapelon et al. 1991; Sibille et al. 1993; Chapelon et al. 1996; Clarke and ter Haar 1997; Chapelon et al. 2000). These studies all contain unambiguous statements recommending actively *avoiding* cavitation when the therapeutic goal is controlled localized heating.

In the preceding list of authors, Lele (1987), Hynynen (1991) and Clarke and ter Haar (1997), as well as Sanghvi et al. (1996), observe cavitation-related enhanced heating – the heating rate measured via single thermocouple during insonation increased dramatically above some threshold insonation pressure, with (in the Lele and Hynynen studies) concomitant dramatic increase in measured acoustic emission. In the Hynynen and Sanghvi studies, regions of enhanced echogenicity in ultrasound images of the focal region were observed. Sanghvi et al. report 'cloud-like' regions of echogenicity that started at the focus and gradually migrated toward the therapy transducer. They were unable to effectively propagate the ultrasound beyond the cloud, a clear indication of bubble activity.

Thus we see that bubbles are important in HIFU applications, and in particular that a bubble-mediated heating effect has been demonstrated in the literature in vivo. It is one aim of the current work to provide a basis for using bubbles to enhance controlled localized heating. It is precisely the fact that bubbles are so efficient at transducing acoustic energy into mechanical energy that motivates the present work.

THE GOOD: ENHANCING RAPID HYPERTHERMIA

We have undertaken a series of laboratory experiments on tissue-mimicking phantoms insonated by 1 MHz focused pulsed ultrasound at MPa pressure amplitudes. The need for independently and simultaneously measured pressures and temperatures, (as opposed to using a derating process to infer the pressure), as well as the ease of instrumentation afforded by cast test samples, motivated the use of a phantom rather than animal tissue. Equally important in our choice of phantoms was the desire to quantitatively model (albeit with Newtonian assumptions) both the acoustic absorption and the bubble dynamics in order to compare to our experiments without employing adjustable parameters – our phantoms allowed us to independently measure both acoustic and thermal material properties to facilitate the partial achievement of this aim.

Experiments

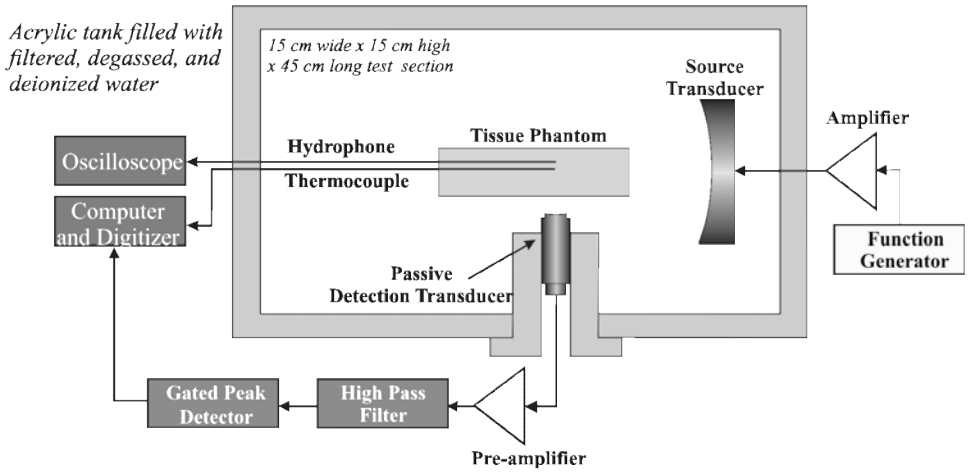

FIGURE 1. Schematic of experimental apparatus, incorporating a 1 MHz focused source, a thermocouple array, a needle hydrophone, and a 15 MHz focused detection transducer

The details of the apparatus and phantoms used in these studies are published elsewhere (Holt and Roy, 2001; Edson 2001; Huang 2002). Figure 1 (from Edson, 2001) depicts the major elements of the insonation geometry and the diagnostic schemes, and is representative of similar setups used in Yang (2002), Holt et al (1998) and Holt and Roy (2001), though the latter 2 did not employ a passive cavitation detector.

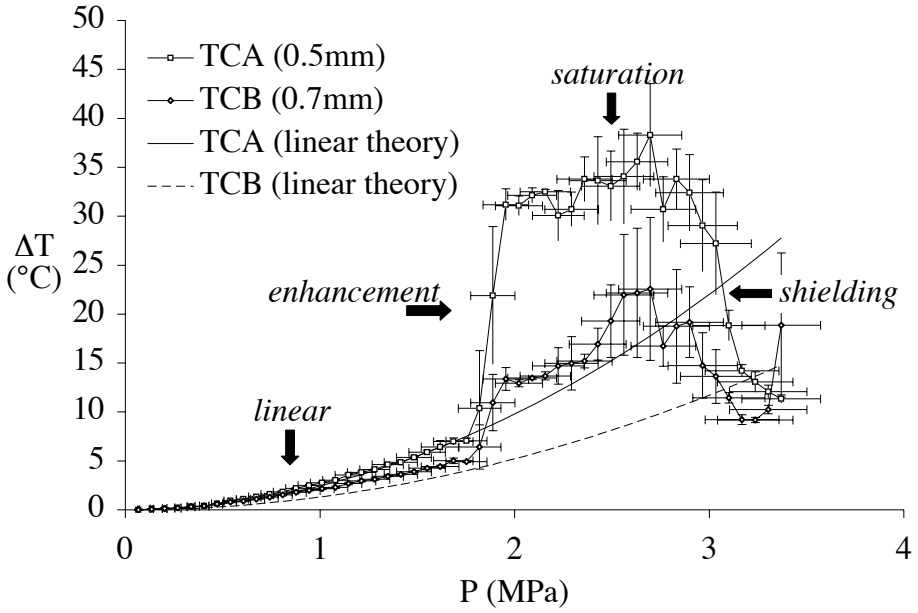

FIGURE 2. Peak temperature increase from ambient vs peak-positive acoustic pressure for an Agar phantom subjected to 0.7 sec 1MHz tonebursts. The thermocouple locations are measured relative to the acoustic axis. The theoretical curves are fit to the data below 1.5 MPa by adjusting the material absorption. Each data point is the mean of 5 runs at that pressure, with 100 sec cooling between runs.

Figure 2 illustrates the typical phenomena associated with the onset of cavitation. For low pressures ("*linear*" in the figure), the temperature rise is governed by linear absorption of the primary 1MHz field, and is linearly proportional to the acoustic intensity, or the square of the acoustic amplitude (Parker 1983; Nyborg 1988; Clarke and ter Haar 1997). Above some critical threshold pressure, the heating increases dramatically *("enhancement*") and becomes rather erratic as indicated by the vertical error bars, which represent the sample standard deviation of 5 runs at each pressure. Upon further increase of the pressure, a *saturation* is often encountered, which may be followed by an actual decrease *("shielding"*) in the peak temperature in the focal region where the thermocouples are located.

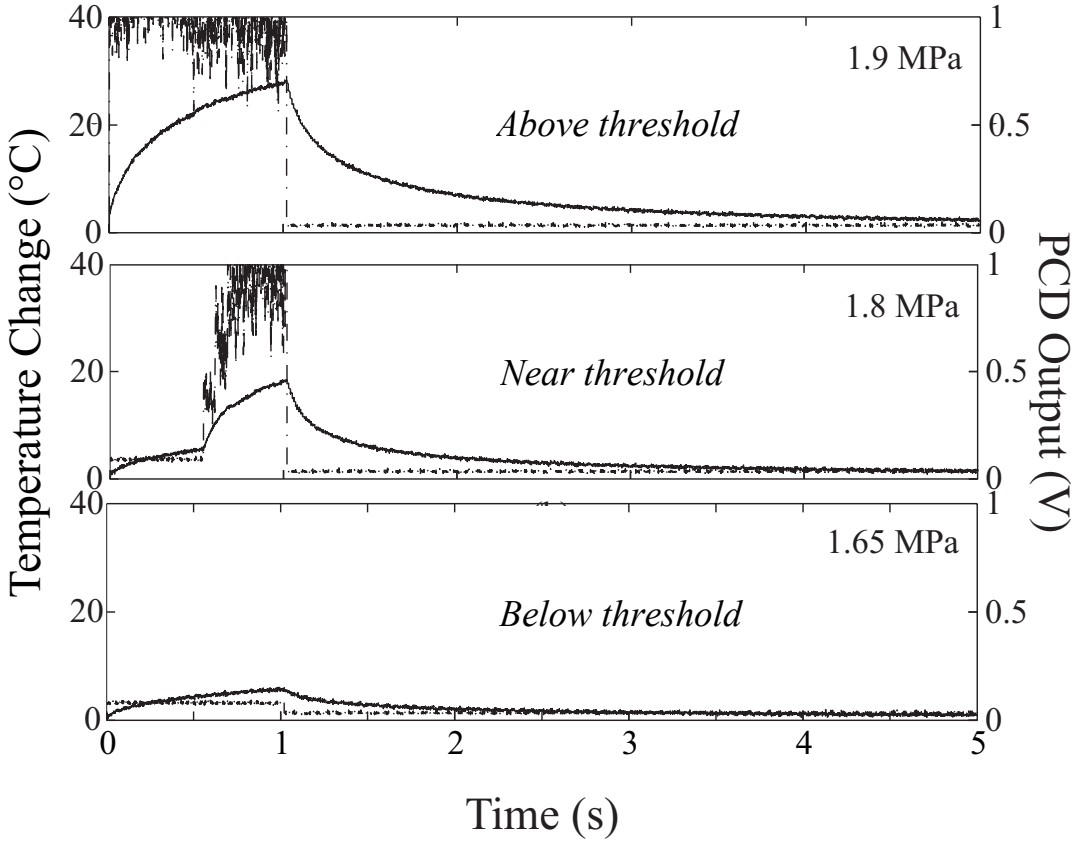

FIGURE 3. Temperature (solid line) and passive cavitation transducer output (dotted line) as a function of time for three 1 sec insonations spanning the threshold pressure for enhanced heating.

Figure 3 illustrates the correlation of broadband noise due to cavitation activity with temperature rise. In all cases, the onset of cavitation activity coincides with the onset of enhanced heating. Not only is this further corroboration of the hypothesis that bubbles are responsible for the enhanced heating seen in Figure 2, but the nature of this mode of detection indicates that at least inertial cavitation (characterized by large expansions followed by violent collapses, see Leighton 1994) is present. This clue is key to our investigation of the bubble size distribution, see below.

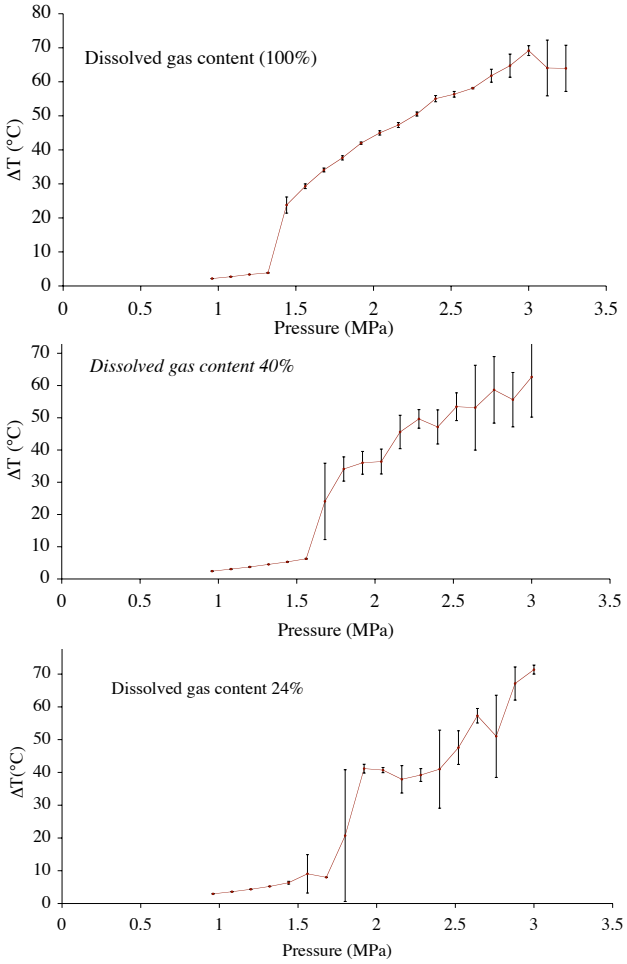

FIGURE 4. Peak temperature rise vs acoustic pressure for different dissolved gas concentrations

Figure 4 illustrates the effect of dissolved gas concentration on bubble-enhanced heating.

Modeling

In an effort to understand the dominant mechanisms responsible for the enhanced heating, we assume, based on the foregoing evidence, that bubbles are responsible for the extra heating. We proceed to build a model for heat deposition in the medium which incorporates contributions from the primary (nonlinear) field, and any bubble sources.

Thermal Sources: Primary Acoustic Absorption, Bubble Viscous Dissipation And Bubble Secondary Acoustic Absorption

The heat conduction equation is solved numerically, with thermal sources due to the primary heating and due to bubble terms (Edson, 2001). Since we are working at 1 MHz, and we infer that most of our bubbles will be less than 50 microns in radius, and also assuming that bubbles remain spherical for most of their lifetime, the 2 dominant bubble terms will come from viscous heating of the external medium, and secondary acoustic heating due to the absorption of the sound actively radiated by the bubble (Holt and Roy, 2001). The heat conduction equation is written in the following form:

$$\rho C \frac{\partial T}{\partial t} = \overbrace{K\nabla^2 T}^{\text{Conduction}} + \overbrace{q_{us} + q^*_{vis} + q^*_{rad}}^{\text{Source/Sink Terms}} \qquad (1)$$

where T is the temperature, ρ the density, C the specific heat, and K the thermal conductivity of the tissue phantom material that we determine independently (Huang, 2002). The source terms are defined as

$$q_{us} = \frac{2\alpha}{\omega^2 \rho c}\left\langle \left(\frac{\partial p}{\partial t}\right)^2 \right\rangle_t ; \qquad (2)$$

q_{us} is the primary acoustic absorption heating term, where a is the absorption, w the frequency of the primary acoustic field, c is the speed of sound, and p is the local acoustic pressure, and the bracket denotes a time average. The pressure is obtained

from the Westerveldt equation (Hamilton and Morfey, 1998) which is solved via a Finite-Difference Time-Domain (FDTD) technique (Hallaj and Cleveland, 1999):

$$\nabla^2 p - \frac{1}{c^2}\frac{\partial^2 p}{\partial t^2} + \underbrace{\frac{2\alpha}{c\omega^2}\frac{\partial^3 p}{\partial t^3}}_{\text{Loss Terms}} + \underbrace{\frac{\beta}{\rho c^4}\frac{\partial^2 p}{\partial t^2}}_{\text{Nonlinear Terms}} = 0, \tag{3}$$

where $\beta = 1\text{-}B/2A$ is the medium nonlinearity coefficient. The bubble viscous heating source term q^*_{vis} is obtained from the viscous dissipation density for a single bubble q_{vis}, given by the following time average (Prosperetti, 1977):

$$q_{vis} = W_{vis} \Big/ V_{eff} \; ; W_{vis} = 16\pi\mu \left\langle R\dot{R}^2 \right\rangle_t, \tag{4}$$

where μ is the phantom shear dynamic viscosity, V_{eff} is an effective volume for the viscous dissipation (approximately $<R>_t$), and the time average of the bubble radius $R(t)$ is computed by solving a version of the Rayleigh-Plesset equation (Keller and Kolodner 1956; Keller and Miksis 1980):

$$\left(1 - \frac{\dot{R}}{c}\right)R\ddot{R} + \frac{3}{2}\dot{R}^2\left(1 - \frac{\dot{R}}{3c}\right) = \left(1 + \frac{\dot{R}}{c}\right)\frac{P\left(R,\dot{R},t\right)}{\rho} + \frac{R}{\rho c}\frac{\partial P\left(R,\dot{R},t\right)}{\partial t} \tag{5}$$

$$P\left(R,\dot{R},t\right) = P_l\left(\frac{R_0}{R}\right)^{3\kappa} + P_v - P_0 - \frac{2\sigma}{R} - \frac{4\mu\dot{R}}{R} - P_a \sin(\omega t) \tag{6}$$

$$P_l = P_0 - P_v - \frac{2\sigma}{R_0}, \tag{7}$$

where κ is the polytropic exponent, σ is the surface tension, P_l is the pressure in the phantom medium, R_0 is the equilibrium radius of a bubble, P_0 is the ambient pressure, P_v is the vapor pressure, and P_a is the acoustic pressure, obtained from Eq. (3). Finally, the bubble secondary acoustic heating source term q^*_{rad} is obtained from the secondary acoustic heating estimate for a single bubble q_{rad}:

$$q_{rad} = \frac{\rho\alpha}{c}\left\langle R\left(2\dot{R}^2 + R\ddot{R}\right)\right\rangle_t, \tag{8}$$

where the absorption coefficient αmay be considered as frequency-dependent (Hilgenfeldt et al., 2000; Edson, 2001) to more accurately account for the absorption of the outgoing shock waves emitted by inertially-collapsing bubbles.

Results: Heating from single bubbles in the parameter space

Equations (1-8) may be integrated to obtain numerical estimates for bubble-induced heating. Before presenting those results, it is of interest to present the underlying bubble response. Figure 5 presents the response of a bubble driven by a 1 MPa, 1 MHz sine wave in the parameter space of bubble size and medium viscosity. Both the absolute maximum radius (5a) and the normalized expansion ratio (5b) are plotted. The nonlinear resonances typical of bubbles are easily identified in (5a), while in (5b) the location of inertially-collapsing bubbles is concident with the single large peak. In both depictions, at low viscosities and near 100 nm bubble sizes, a critical radius (corresponding to a quasi-static Blake threshold) below which the bubble response is negligible due to the effect of surface tension.

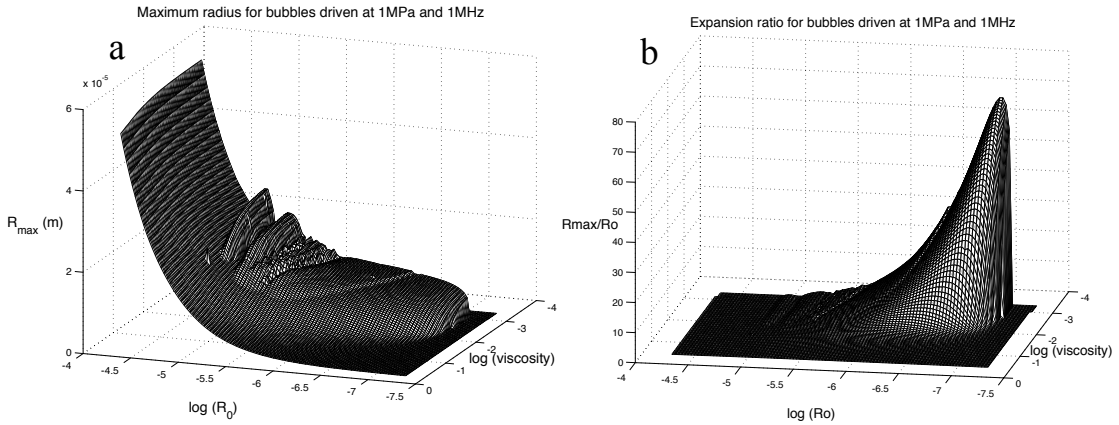

FIGURE 5. Maximum radius (a) and expansion ratio R_{max}/R_0 (b) for bubbles driven at 1 MPa and 1 MHz vs bubble equilibrium size R_0 and host medium shear dynamic viscosity μ..

Figure 6 plots the calculated contributions of viscous heating (Eq. (4)) and secondary acoustic heating (Eq. (8)) for the same parameter space (but slightly higher pressures) as in Figure 5. Fig. 6a shows a global maximum for the viscous source power for large viscosity and intermediate bubble size, corresponding to a noninertial response in Fig. 5; Fig. 6b indicates that the maximum power developed by the secondary acoustic emission mechanism is due to inertially-collapsing bubbles, corresponding to the peak in Fig. 5b (shifted to smaller bubble sizes in 6b due to the higher pressure used).

FIGURE 6. Single bubble heating contributions for a 1MHz, 2.8 MPa acoustic pressure. Viscous power (a) and secondary acoustic absorption power (b) are plotted vs bubble size and phantom viscosity.

If we choose 'optimal' bubble sizes for each type of contribution, then the optimal viscous source bubble would be roughly 4 μm at 0.07 Pa-s viscosity. The optimal secondary acoustic or inertial bubble would be say 200 nm at 0.003 Pa-s. We can then define the source strengths $q^*_{vis,rad}$ in Eq. (1) as $Nq_{vis,rad}$, where N is the number of bubbles in the focal region required to make up the difference between the primary acoustic heating and the bubble-enhanced heating observed in a situation as depicted in Fig. 2. Table 1 illustrates the results of such a calculation for a typical run:

TABLE 1. Number of bubbles required to achieve experimentally observed ΔT

Acoustic Pressure (MPa)	Experiment ΔT (°C)	Number of optimal viscous bubbles	Number of optimal inertial bubbles
2.06	6.8	10	10
2.18	8	12	12
2.30	10	16	15
2.41	12	17	16
2.53	15	22	22
2.64	21	27	28
2.76	24	35	35

It is rather striking that no more than 35 'optimal' bubbles would be required to generate an extra 24°C temperature rise. Certainly 35 is not to be taken exactly, but the order of magnitude is correct.

THE BAD: WHAT WE DON'T KNOW

Bubble Size Distribution

Our working hypothesis is that sufficient nuclei (hydrophobic inclusions, or possibly even stabilized microbubbles) exist in our phantoms such that, above a threshold pressure amplitude, acoustic cavitation occurs. The distribution of bubble sizes is, however, unknown. The nuclei most susceptible to inertial cavitation at 1 MHz will possess an equilibrium radius R_0 of order 0.1 μm (Apfel and Holland 1991; Allen et al. 1997), and one might guess at an initial distribution centered on this size. But over the course of a typically 1-sec long insonation, the size distribution will evolve, eventually resulting in an asymptotic bubble size distribution. Imaging these bubbles via ultrasound or optics is not feasible, at least in these phantoms. Below we discuss a method to narrow down the possible bubble size distributions.

Tissue and Tissue-Mimicking-Phantom Viscosity

The Agar phantoms we use (as well as most biological fluids and tissues) exhibit viscoelastic properties, and we should properly be using a model of the host medium which possesses such features. We can reasonably assume that at the extremely high strain rates typical of nonlinear bubble oscillations at MHz frequencies we will reside in the high-frequency asymptote for the shear viscosity number. This is important because the asymptotic value of the shear viscosity number is determined by shear thinning, and will in general be orders of magnitude below the static or low-strain-rate value. This still leaves us with some uncertainty regarding the shear viscosity of our Agar phantoms. We can invert the well-known expression relating the measured acoustic absorption (18 Np/m/MHz) to the shear dynamic viscosity to obtain a value of 3.15 Pa-s (water is 10^{-3} Pa-s, and whole blood at body temperature has a measured value of ~5 x 10^{-3} Pa-s.). In light of the above discussion of the viscoelastic nature of our phantom 3.15 Pa-s should be considered an extreme upper bound, while water (0.001 Pa-s) should be considered a lower bound. We note that, in light of the results from our passive cavitation detector in Fig. 3, we expect that we indeed have bubble sizes near 1 micron, and a viscosity value on the order of 0.005 Pa-s.

THE UGLY (BUT USEFUL): HOW WE DETERMINE WHAT WE DON'T KNOW

Growth by rectified diffusion (Eller and Flynn 1965; Crum and Hansen, 1982; Church 1988)) will shift the mean of the bubble size distribution to larger radii over a long time scale of hundreds to thousands of acoustic cycles. Bubble growth will be

interrupted by: (1) the onset of shape instabilities leading to breakup of the bubble (Eller and Crum 1970; Brenner et al. 1995; Gaitan and Holt 1999; Hao and Prosperetti 1999) or, (2) the diminution of bubble response as the mean bubble size increases well past the regime of resonant behavior such that bubble growth by rectified diffusion is halted.

By coupling Eqs. (5-7) with the equations for shape and diffusive stability, we may then place further bounds on bubble sizes and medium viscosities. Without reproducing the equations here (for details see the above references, as well as Yang, 2002), we present results for shape instabilities and rectified diffusion equilibria in our parameter space. Figure 7 shows the mass diffusion equilibrium (threshold for growth by rectified diffusion) and the shape instability boundary in the parameter space. Bubbles to the left of the diffusion equilibrium will grow, bubbles to the right will dissolve. Bubbles above the shape instability boundary are stable with respect to perturbations from sphericity, while below the boundary they are unstable, and will rapidly exhibit large amplitude shape oscillations and subsequent breakup. Thus, the allowed region for bubbles is the shaded wedge shape, with asymptotic bubble size distributions to be expected near the rightmost boundary of the wedge.

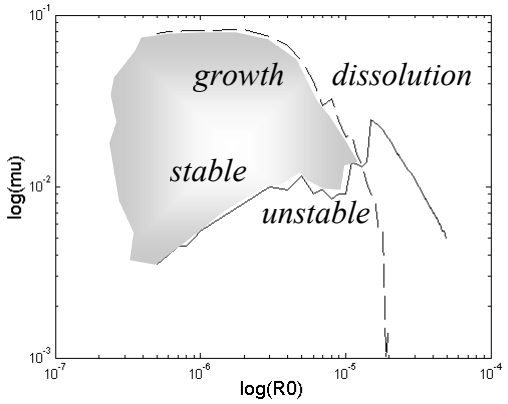

FIGURE 7. Thresholds for growth by rectified diffusion (dotted line) and onset of shape instability (solid line) for the most unstable modes. Calculations are for 1 MHz and 2.0 MPa, and a dissolved gas content of 10% of saturation.

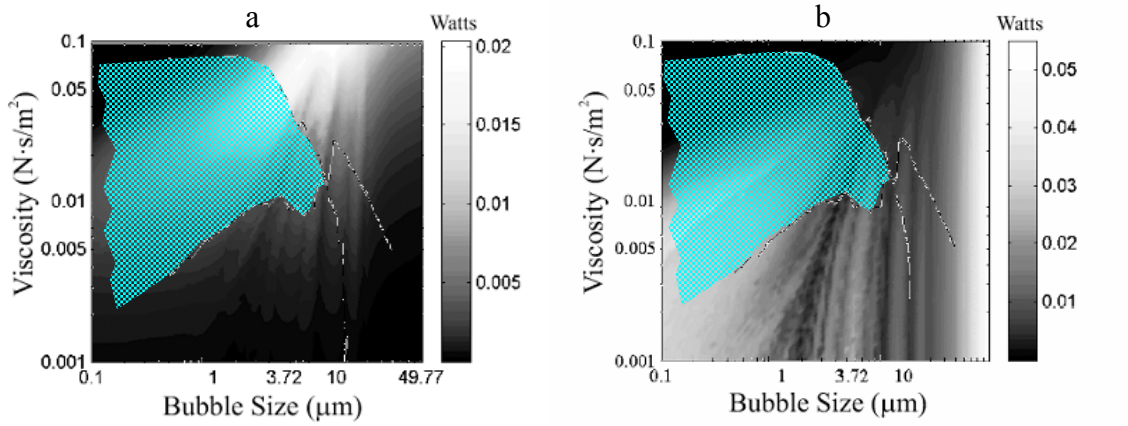

is most likely near 0.005.

OUTLOOK AND FUTURE WORK

The above results indicate that we can expect to quantitatively model bubble-enhanced heating in a predictive way. We need further experiments to verify the predictions of our instability models for bubble-size distributions. With such a validated model, it may be possible in the future to ensure that HIFU parameters are chosen in order to maximize the efficiency benefit of bubble-enhanced heating; conversely, such a model (perhaps also combined with a passive cavitation monitoring capability) could ensure the avoidance of cavitation which would go undetected using conventional ultrasound imaging.

ACKNOWLEDGMENTS

We gratefully acknowledge the support of DARPA (via a subcontract to the University of Washington) and the U.S. Army (via a subcontract to the National Center for Physical Acoustics). X. Yang was partially supported by NASA.

REFERENCES

1. Allen JS, Roy RA, Church CC. IEEE UFFC 1997; 44:743-751
2. Apfel RE, Holland CK. Ultrasound Med. Biol. 1991; 17:179-181
3. Arefiev A, Prat F, Chapelon J-Y, Tavakkoli J, Cathignol D. Ultrasound Med. and Biol. 1998; 24:1033-1043.
4. Bacon DR, Carstensen EL. J. Acoust. Soc. Am. 1990; 88:26-34
5. Brenner MP, Lohse D, Dupont TF. Phys. Rev. Lett 1995; 75:954-957
6. Bush NL, Rivens I, ter Haar GR, Bamber JC. Ultrasound Med. Biol. 1993; 19:789-801
7. Carstensen EL, Kelly P, Church CC, et al. Ultrasound Med. and Biol. 1993; 19:147-165
8. Chapelon J-Y, Cathignol D, Cain C, Ebbini E, Kluiwstra J-U, Sapozhnikov OA, Fleury G, Berriet R, Chupin L, Guey J-L. Ultrasound Med. and Biol. 2000;26:153-159
9. Chapelon J-Y, Dupenloup F, Cohen H, Lenz P. IEEE UFFC 1996; 43:623-625
10. Chapelon J-Y, Prat F, Delon C, Margonari J, Gelet A, Blanc E. Proc. IEEE Ultrason. Symp. 1991; 1357-1360
11. Chavrier F, Chapelon J-Y, Gelet A, Cathignol D. J. Acoust. Soc. Am. 2000;108:432-440.
12. Christopher T, Carstensen EL. Ultrasound Med. Biol. 1996; 22:1103-1116
13. Church CC. J. Acoust. Soc. Am. 1988; 83:2210-2217.
14. Clarke RL, ter Haar GR. Ultrasound Med. Biol. 1997; 23:299-306
15. Crum LA, Hansen GM. Phys. Med. Biol. 1982; 27:413-417
16. Damianou CA, Sanghvi NT, Fry FJ, Maass-Moreno R. J. Acoust. Soc. Am. 1997; 102:628-634
17. Dalecki D, Carstensen EL, Parker KJ. J. Acoust. Soc. Am. 1991; 89:2435-2447
18. Ebbini ES, ed. Special issue on therapeutic ultrasound. IEEE Trans UFFC 1996; 43:989-1129.
19. Edson, PL. The role of acoustic cavitation in enhanced ultrasound-induced heating in a tissue-mimicking phantom. PhD dissertation, Boston University, Boston, Massachusetts, 2001.
20. Eller, A, Flynn HG. J. Acoust. Soc. Am. 1965; 37:493-503
21. Eller A, Crum LA. J. Acoust. Soc. Am. 1970; 47:762-767
22. Everbach EC, Makin IRS, Azadniv M, Meltzer RS. Ultrasound Med. and Biol. 1997; 23; 619-624
23. Fowlkes JB, Holland CK. Mechanical Bioeffects from Diagnostic Ultrasound: AIUM Consensus Statements. J. Ultrasound Med. 2000; 19. (special issue)
24. Fry FJ, Kossoff G, Eggleton RC, Dunn F. J. Acoust. Soc. Am. 1970;48:1413-1417.
25. Fry FJ, Sanghvi T, Foster RS, et al. Ultrasound Med. and Biol. 1996;21:1227-1237
26. Fry WJ, Wulff VJ, Tucker D, Fry FJ. J. Acoust. Soc. Am. 1950; 22:867-876.

27. Gaitan, DF, Holt, RG. Phys. Rev. E 1999; 59:5495-5502
28. Goss, S.A., Johnson, R.L. and Dunn, F. J. Acoust. Soc. Am. 1978; 64:423-457.
29. Goss, S.A., Johnson, R.L. and Dunn, F. J. Acoust. Soc. Am. 1980; 68:93-108.
30. Hallaj IM, Cleveland RO. J. Acoust. Soc. Am.1999;105(5):L7-L12
31. Hamilton MF, Morfey CL. Model equations. In: Hamilton MF, Blackstock DT, editors. Nonlinear Acoustics. New York: Academic Press; 1998.
32. Hao Y, Prosperetti A. Phys. Fluids 1999; 11:1309-1317
33. Hilgenfeldt S, Lohse D, Zomack M. J. Acoust. Soc. Am. 2000; 107:3530-3539.
34. Holt RG, Cleveland RO, Roy RA. Proc. of the 16th ICA/135th Meeting of the ASA, Seattle, WA, P. Kuhl and L. Crum, eds., (ASA, New York, 1998), 1057-1059
35. Holt, RG, Roy, RA. Ultrasound Med. Biol. 2001; 27:1399-1412.
36. Huang, J. Heating in vascular tissue and flow-through tissue phantoms induced by focused ultrasound. PhD dissertation, Boston University, Boston, Massachusetts, 2002.
37. Hynynen K. Ultrasound Med. Biol. 1991; 17:157-169
38. Hynynen K, Jolesz F. Ultrasound Med. Biol. 1998; 24:275-283
39. Kamath V, Oguz HN, Prosperetti A. J. Acoust. Soc. Am. 1992; 92:2016-2023
40. Keller, JB, Kolodner, II. J. Appl. Phys. 1956; 27:1152-1161
41. Keller, JB, Miksis, MJ. J. Acoust. Soc. Am. 1980; 68:628-633
42. Lehmann JF, Herrick, JF. Arch. Phys. Med. Rehab. 1953; 34:86-98
43. Leighton, TG. The acoustic bubble. London: Academic Press 1994:291-298
44. Lele PP. Effects of ultrasound on solid mammalian tissues and tumors in vivo. In Repacholi MH, Grandolfo M, Rindi A, eds. Ultrasound: Medical applications, biological effects and hazard potential. New York: Plenum 1987:275-306
45. Nyborg WL. Phys. Med. Biol. 1988; 33:785-792
46. Parker KJ. J. Acoust. Soc. Am. 1983; 74:1356-1361
47. Penney DP, Schenk EA, Maltby K, et al. Ultrasound Med. and Biol. 1993; 19; 127-135
48. Prosperetti A. J. Acoust. Soc. Am. 1977; 61:17-27
49. Prosperetti A. J. Fluid Mech. 1991; 222:587-616
50. Sanghvi NT, Fry FJ, Bihrle R, Foster RS, Phillips MH, Syrus J, Zaitsev AV, Hennige CW. IEEE Trans UFFC 1996; 43:1099-1109.
51. Sibille A, Prat F, Chapelon J-Y, El Fadil FA, Henry L, Theilliere Y, Ponchon T, Cathignol D. Ultrasound Med. and Biol. 1993;19:803-813
52. Smith NB, Hynynen K. Ultrasound Med. and Biol. 1998;24:1045-1054
53. Tavakkoli J, Birer A, Arefiev A, Prat F, Chapelon J-Y, Cathignol D. Ultrasound Med. and Biol. 1997; 23:107-115
54. ter Haar GR. Ultrasound Med. and Biol. 1995; 21:1089-1100
55. ter Haar GR, Daniels S, Eastaugh KC, Hill CR. Br. J. Cancer 1982; 45 (Suppl. V):151-155
56. Vaezy S, Martin R, Schmiedl U, et al. Ultrasound Med. and Biol. 1997; 23:1413-1420
57. Vaezy S, Martin R, Yaziji H, et al. Ultrasound Med. and Biol. 1998; 24:903-910
58. Williams AR, Kubowicz G, Cramer E, et al. Echocardiography 1991; 8:423-433
59. Yang, X. Investigation of bubble dynamics and heating during focused ultrasound insonation in tissue mimicking materials. PhD dissertation prospectus, Boston University, Boston, Massachusetts, 2002.